

Supporting Information

Improved photoelectrochemical performance of electrodeposited metal-doped BiVO₄ on Pt-nanoparticle modified FTO surfaces

Ramona Gutkowsk^a, Daniel Peeters^b and Wolfgang Schuhmann^{a,*}

^a Analytical Chemistry - Center for Electrochemical Science (CES), Ruhr-Universität Bochum, Universitätsstr. 150, D-44780 Bochum, Germany

^b Inorganic Chemistry II, Ruhr-Universität Bochum, Universitätsstr. 150, D-44780 Bochum, Germany

Characterization of BiVO₄ samples. UV-vis spectra were recorded with a Varian Carry 500 UV-Vis spectrometer with integrated sphere and reflection mode. For X-ray diffraction (XRD) analysis a Bruker D8 Advance AXS diffractometer operating with Cu K α radiation ($\alpha = 1.5418 \text{ \AA}$) equipped with a position sensitive detector (PSD) was used. All samples were analysed in θ -2 θ geometry. Raman spectroscopy was performed using a Jobin-Yvon iHR550 (Bensheim, Germany) spectrometer with a 532 nm Ventus laser (Laser Quantum, Stockport, UK) and a power of 2 mW. For each sample at least 20 points were measured in a row by a fixed plate on a x,y-positioning system with integrated step-motors. The spectra shown in Figure S5 represent the average of all measured 20 points for each sample. Using scanning electron microscopy (SEM) and energy-dispersive X-ray (EDX) measurements the morphology, the film thickness and the element distribution on the different doped BiVO₄ films on FTO substrates were investigated using an eSEM Dual Beam Quanta 3D FEG SEM with an energy diffraction X-Ray analysis system (Genesis XM2i).

Evaluation of the Pt-nanoparticle loading. The loading of Pt-nanoparticles on FTO was controlled by applying sequences of the potential pulse profile (0 V for 1 s, -1 V for 0.2 s vs. Ag/AgCl/3 M KCl) from a 0.4 mM H₂PtCl₆ solution. Using the hydrogen evolution reaction (HER) the correlation between Pt-nanoparticle loading and the number of applied pulse sequences was demonstrated. 0.1 M Na₂SO₄ (pH = 6) was saturated with Argon. Linear sweep measurements were carried out in a three-electrode set-up with a Ag/AgCl/3 M KCl as a reference electrode and a Nickel foil (99.2 % purity) as counter electrode. Preconditioning was performed by means of cyclic voltammetry using a scan rate of 100 mV/s. The CVs were repeated until no changes were observed. Linear sweep voltammetry was performed with a scan rate of 5 mV/s. All potentials were corrected for the uncompensated resistance (R_u), according to $E_{(iR\text{-corrected})} = E_{(RHE)} - (i_{\text{measured}} \cdot R_u)$.

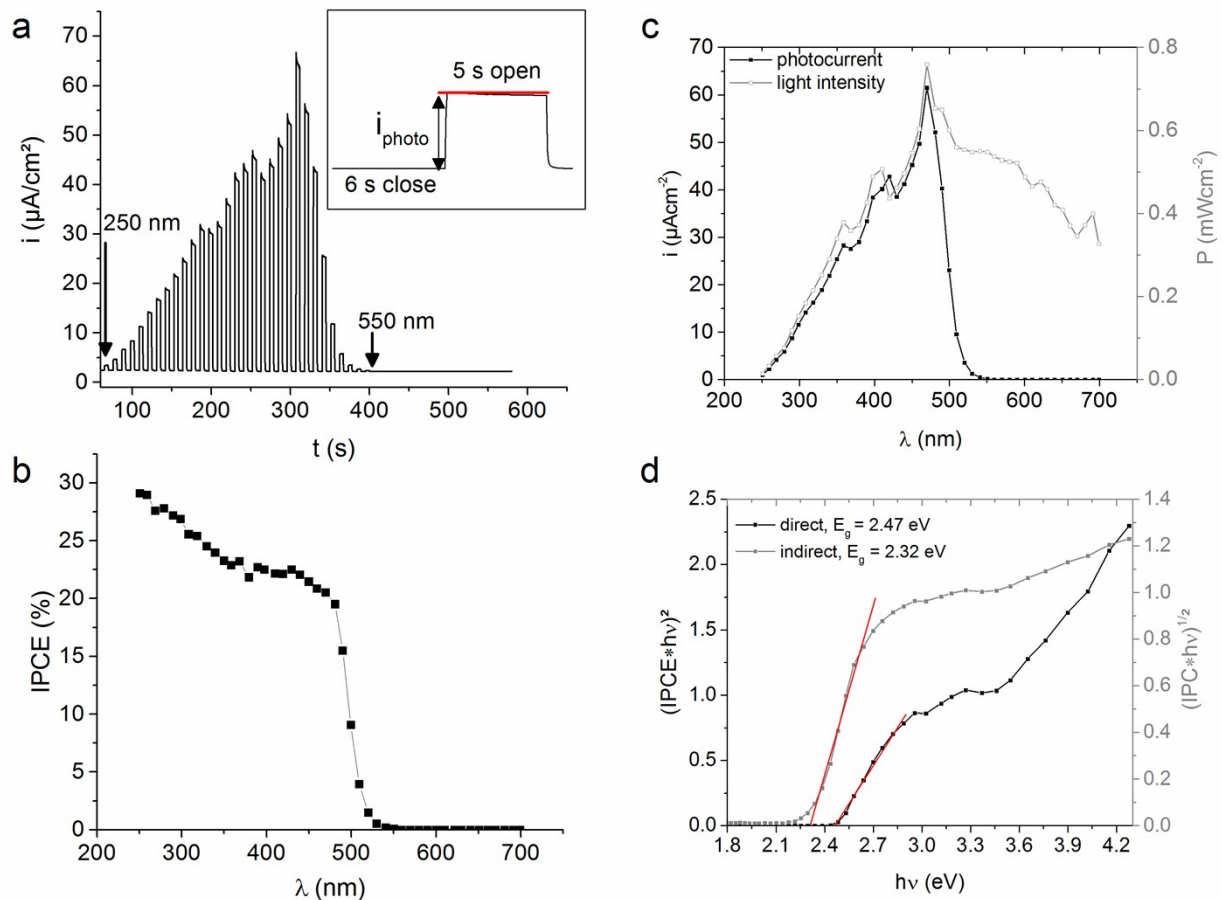


Figure S1: Current-time response for Mo-doped BiVO_4 on Pt-NPs modified FTO at a bias potential of 1.2 V vs. RHE in 0.1 M Na_2SO_4 starting at 250 nm. Shutter is opened for 5 s and closed for 6 s (a). The photocurrent (b) was obtained by subtracting the dark current from the current under illumination (last point before closing the shutter and steady state current was reached, insert in a). Photocurrent and light intensity depending on the wavelength (b), calculation of the IPCE (c) and determination of the band gap using Tauc-plots (d) are shown. Assuming an indirect band gap (c) the results conform to the observed photocatalytic activity until 530 nm (c).

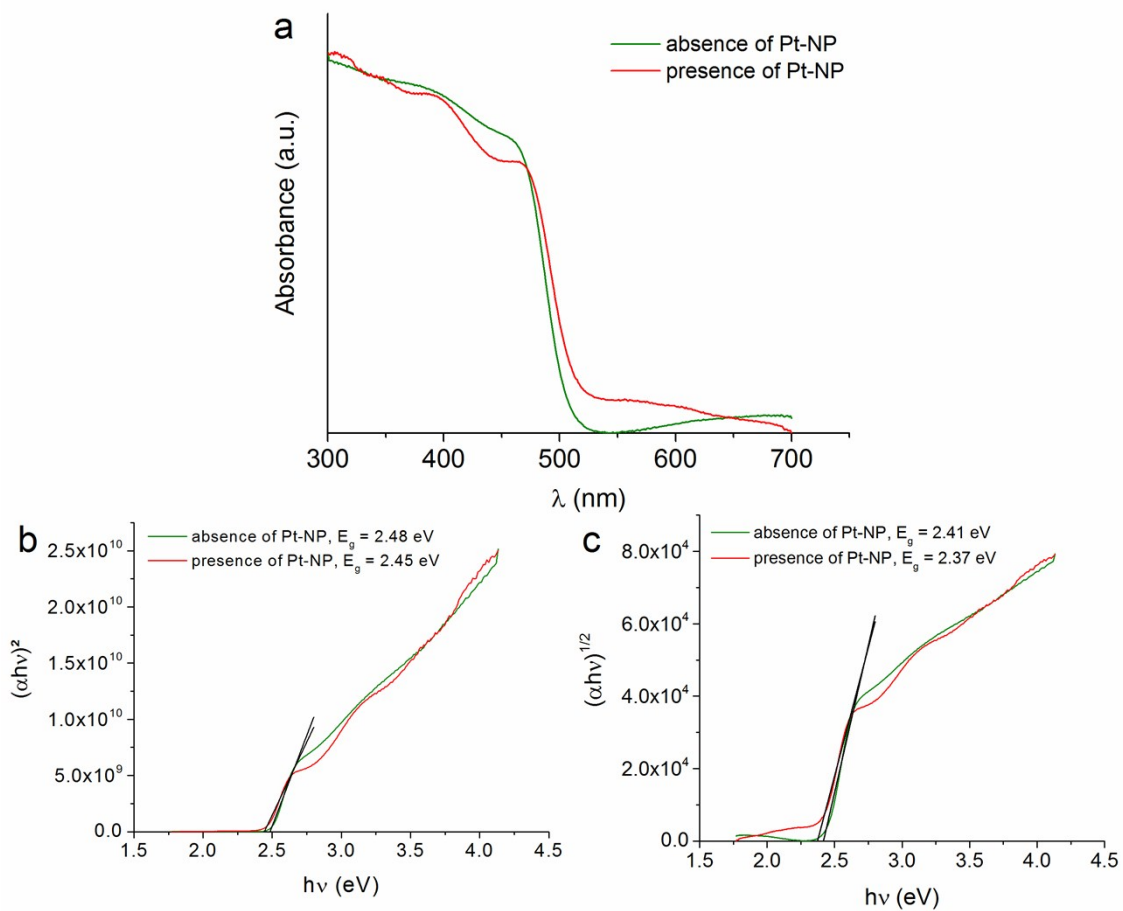


Figure S2: UV-vis absorption spectra of Mo-doped BiVO_4 (layer thickness 600 ± 50 nm) in presence and in absence of Pt-NP (a). Tauc plots for direct (a) and indirect (b) band-to-band transition. The UV-vis spectra coincide with the IPCE spectra in Figure S1.

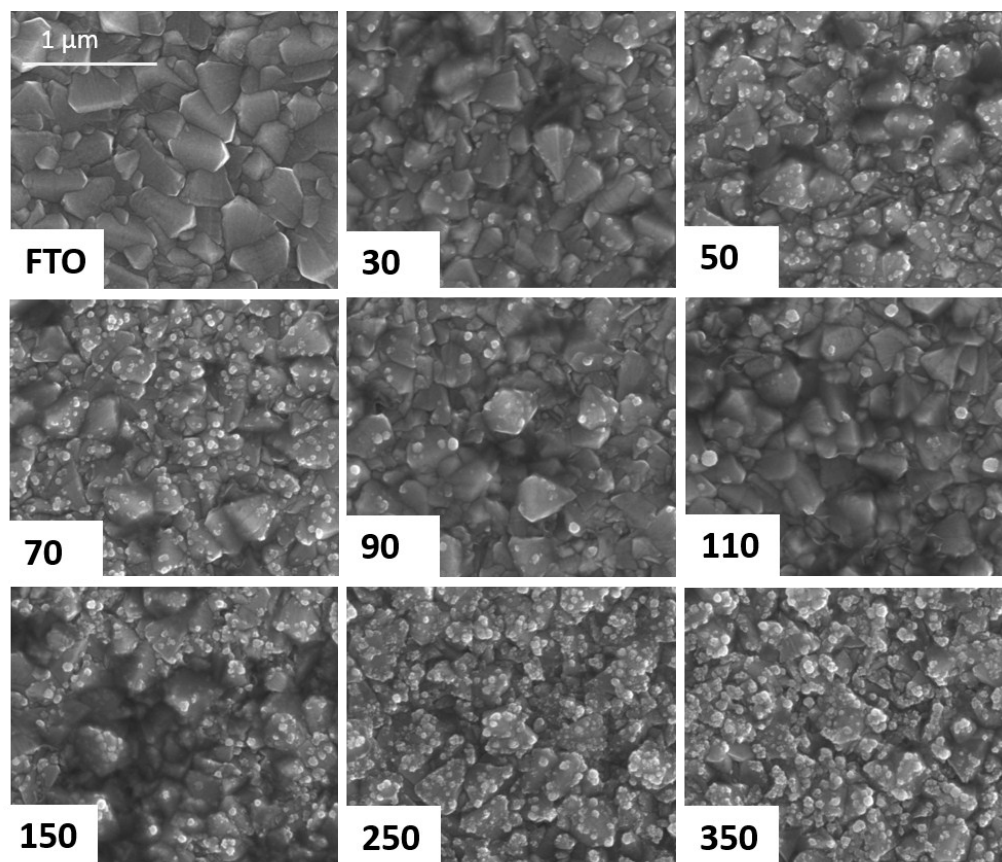


Figure S3: SEM images for electrochemical induced deposition of Pt-nanoparticles in dependence of the number of potential pulse sequences (0.4 M H_2PtCl_6 ; potential pulses: 0 V for 1 s, -1 V for 0.2 s).

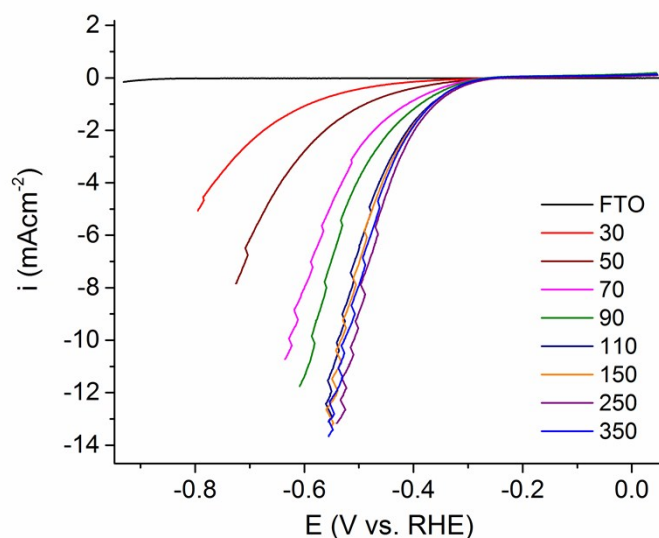


Figure S4: Linear sweep voltammograms for FTO surfaces modified with increasing loading with Pt-nanoparticles in Argon saturated 0.1 M Na_2SO_4 (pH = 6) at a scan rate of 5 mV/s. The loading of the Pt-nanoparticles was changed with increasing the number of potential pulse sequences from 30 to 350 repetitions in comparison to the unmodified FTO. The HER is improved until a maximum loading is reached at 110 sequences. A further increase in the Pt-nanoparticle loading (150, 250 and 350 potential pulse sequences) does not further enhance the HER performance.

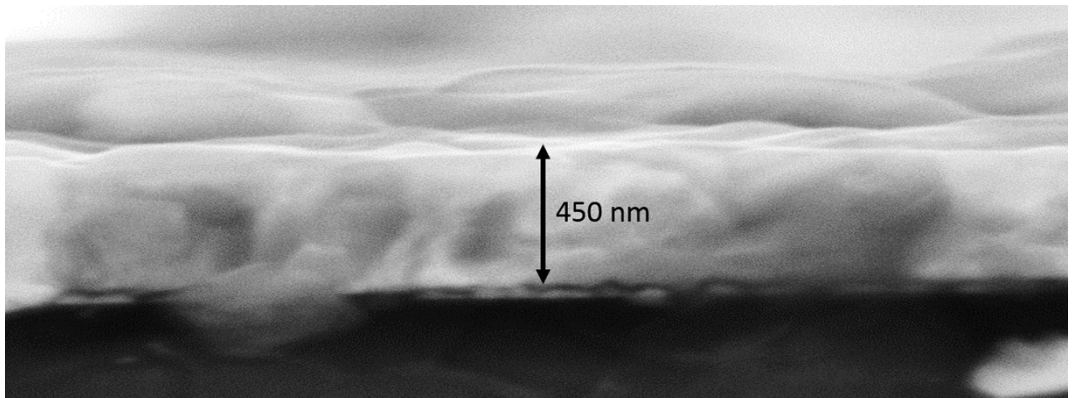


Figure S5: SEM cross section of Mo-doped BiVO₄ deposited on top of Pt-nanoparticles for 400 s. The layer thickness was determined to be about 450 nm ± 50 nm.

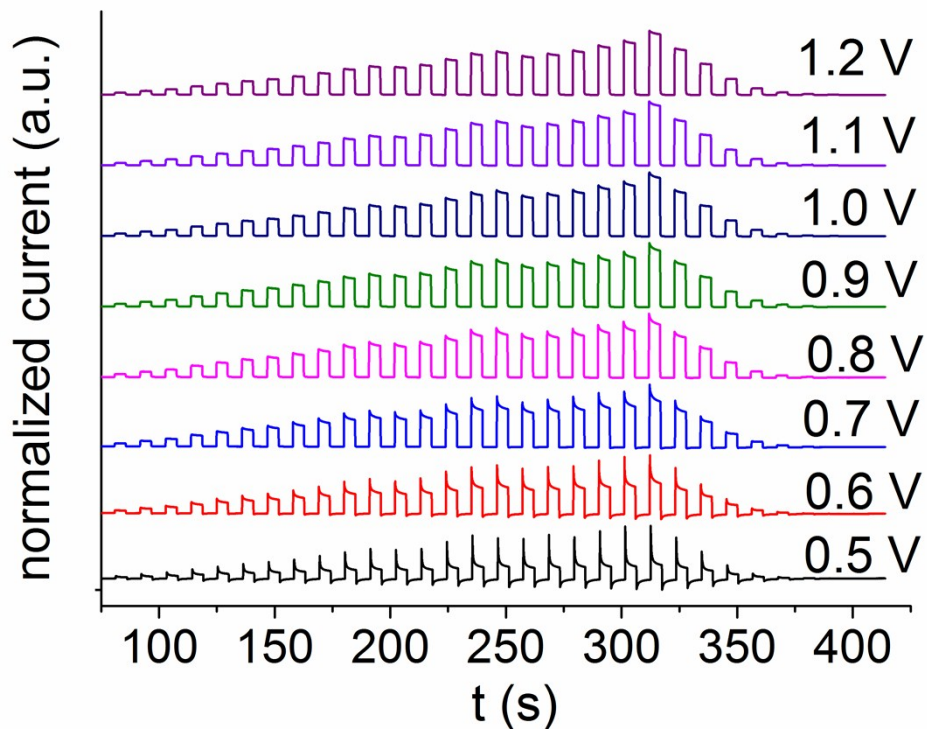


Figure S6: Normalized current vs. time plots at different bias potentials (vs. RHE) in 0.1 M Na₂SO₄ of Mo-doped BiVO₄ film deposited on Pt-nanoparticle modified FTO. The current was normalized to point out the decrease of the initial current peak (when the shutter is opened) and the steady-state current (current after further illumination) at different bias potentials.

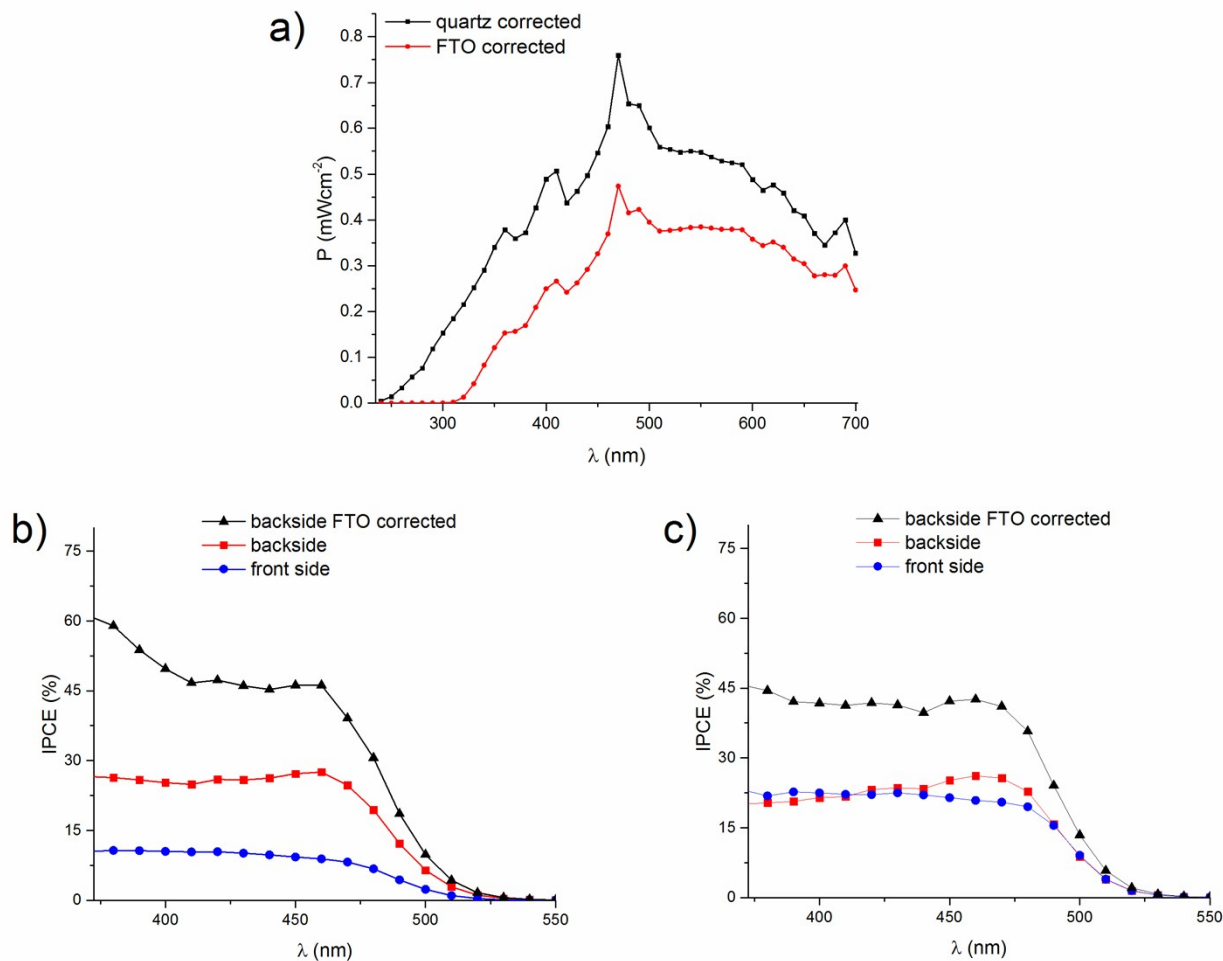


Figure S7: Power density for the incident light with correction of intensity losses through the quartz window or FTO (thickness 2.3 mm) (a). In absence of Pt-NP. (b) The IPCE difference between front side and backside illumination (FTO corrected) is over 35 %. While the IPCE difference between front and backside illumination for Mo-doped BiVO₄ films on top of Pt-nanoparticles (c) with the same layer thickness is only around 20 %. Since no corrections were performed taking into consideration the intensity losses by the electrolyte, higher differences between quartz corrected and FTO corrected power density are expected. If, e.g., the intensity for front-side illumination is corrected also by losses from the electrolyte higher IPCE values are reached. Thus, the error by correcting the FTO power density for thick FTO substrates leads to underestimated IPCE values. Therefore, power correction was not performed, however, clear differences between front and backside illumination in presence and in absence of Pt-NP are demonstrated.

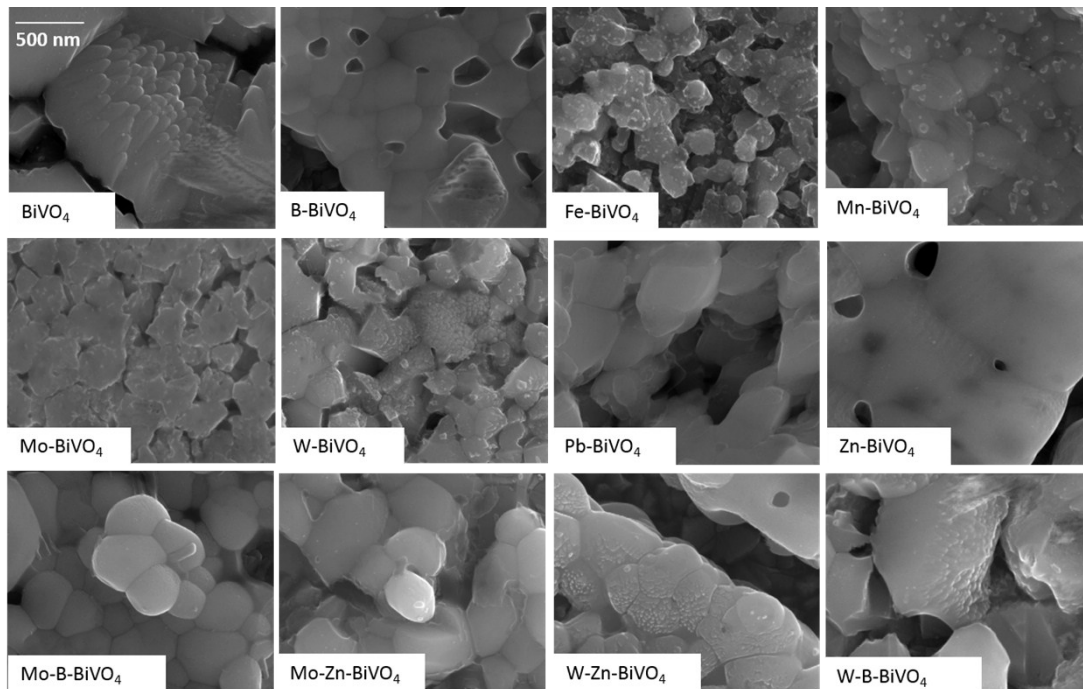


Figure S8: SEM images of pristine BiVO_4 , single and co-doped BiVO_4 films after annealing in air at $500\text{ }^\circ\text{C}$ for 1 h. BiVO_4 has a rough surface. Doping with Mo, Mo/Zn and Mo/B leads to round particles with a homogeneous surface. Doping with W/Zn formed rounder particles as compared to BiVO_4 but with a rough surface. The particles size and surface change with doping.

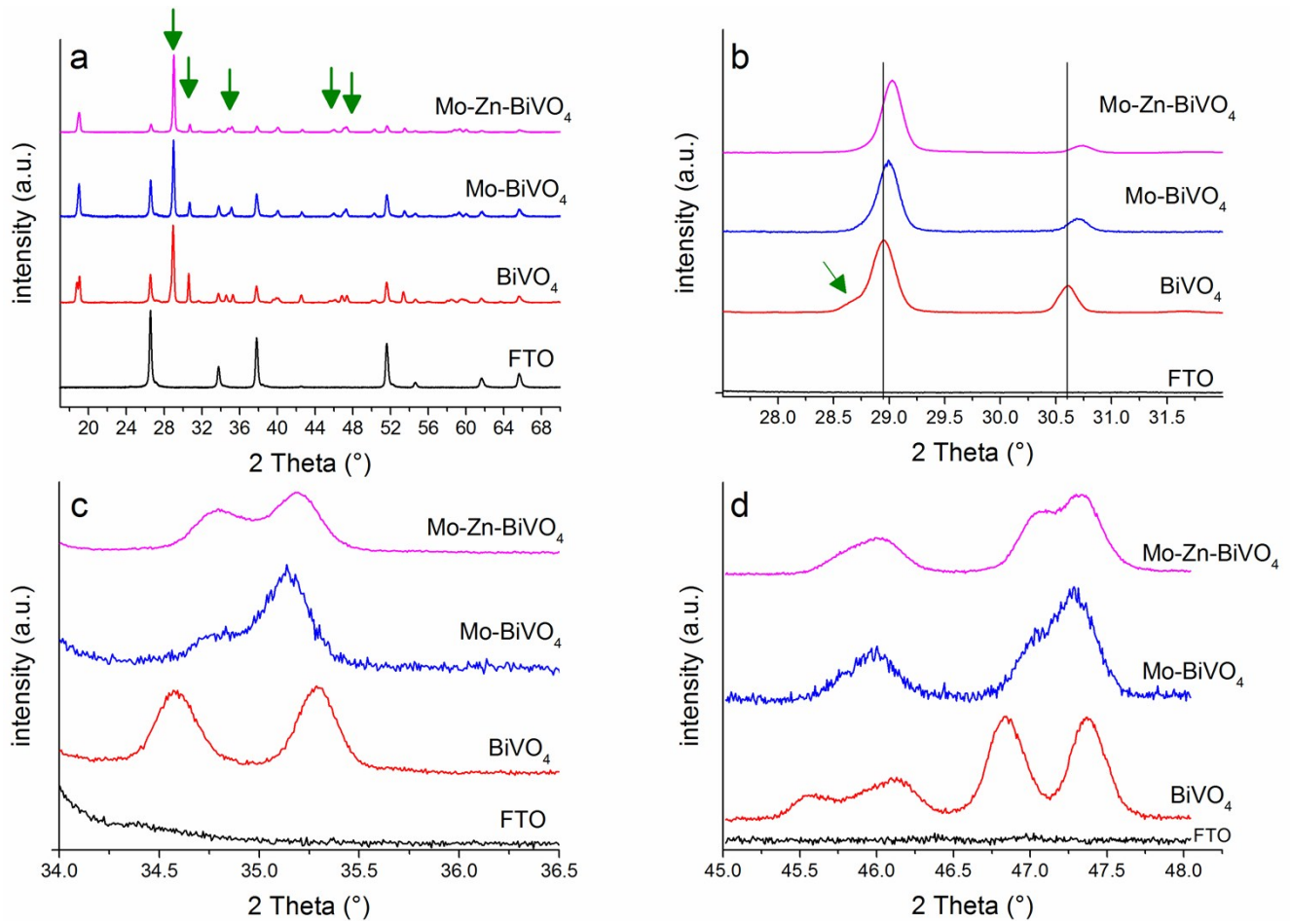


Figure S9: XRD patterns of un-doped and doped BiVO_4 (a). The arrows indicate the position for zooming in (b-d) to more clearly show the peak shift due to doping.

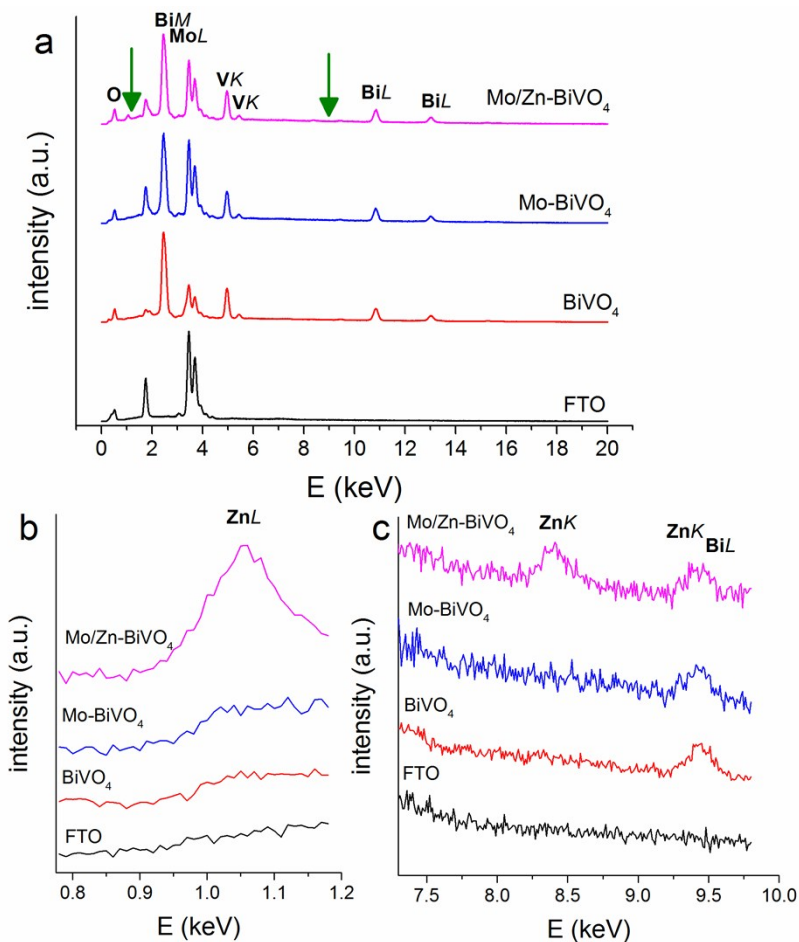


Figure S10: EDX spectrum of BiVO₄ and doped BiVO₄ electrodeposited with Pt-core (a). FTO spectrum was used as reference. BiM and MoL peaks are overlapping. By zooming in at around 1.05 eV a small Zn-peak is observed for Mo/Zn doped BiVO₄ (b). Additionally very small peaks at 8.5 eV and 9.5 eV are detected for Mo/Zn-doped BiVO₄ (c). The peak at 9.5 eV is overlapping with the BiL peaks and observed also in undoped and Mo-doped BiVO₄. The Zn-concentration was quite low and difficult to detect.

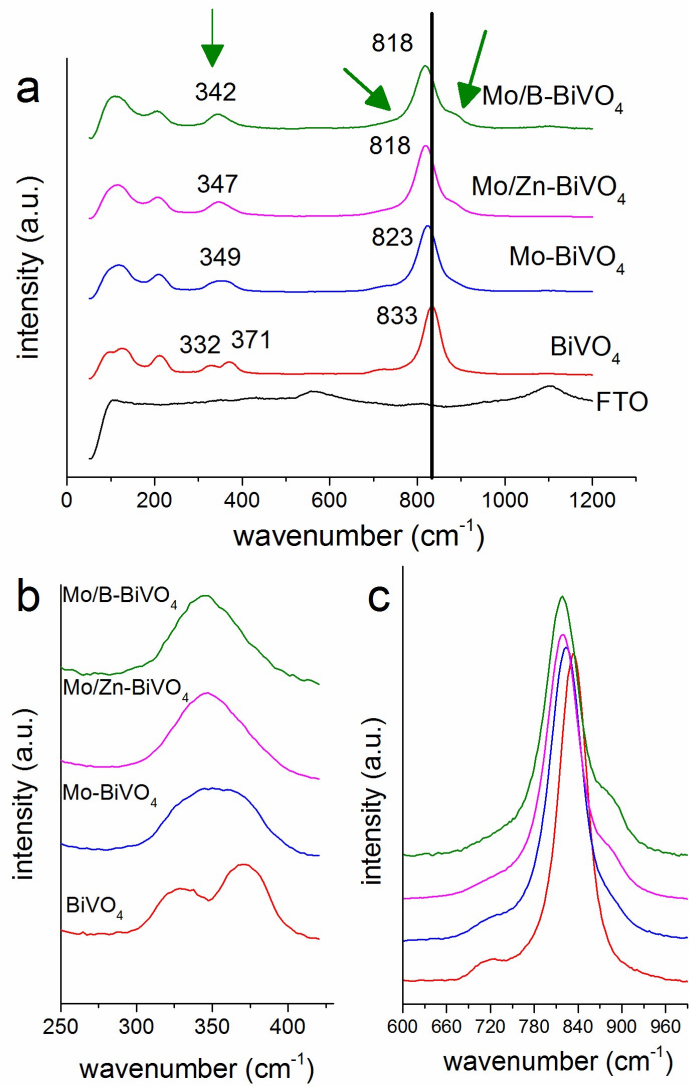


Figure S11: Raman spectra of electrodeposited BiVO₄ samples and doped BiVO₄ samples on FTO substrates modified with Pt-nanoparticles (a). FTO spectrum as a reference. The characteristic peak at 833 cm⁻¹ for the V-O symmetric stretching shifted to lower wavenumbers. After doping the BiVO₄ films with Mo, Mo/Zn or Mo/B the peaks at 340 and 360 cm⁻¹ merged into one peak indicating a deformation of the structure by doping (b). By doping the BiVO₄ the shoulder at 720 cm⁻¹ disappears, while by Mo-doping a shoulder around 870 cm⁻¹ is formed, which can be attributed to Mo-O-Mo stretching.¹

1. V.I. Merupo, S. Velumani, G. Oza, M. Makowska-Janusik, A. Kassiba, *Mater. Sci. Semicond. Process.*, 2015, **31**, 618-623